10th IMC
10th International Masonry Conference
G. Milani, A. Taliercio and S. Garrity (eds.)
Milan, Italy, July 9-11, 2018

DIAGNOSTIC INVESTIGATIONS AND STRUCTURAL HEALTH STATE ASSESSMENT OF SAN PIETRO BELL TOWER IN PERUGIA

P.F. Giordano[1], F. Ubertini[2], N. Cavalagli[2], A. Kita[2], L.F. Ramos[3], M.G. Masciotta[3]

[1] Politecnico of Milano
Department of Architecture, Built environment and Construction Engineering,
Piazza Leonardo da Vinci 32, 20133 Milan, Italy
pierfrancesco.giordano@polimi.it

[2] University of Perugia
Department of Civil and Environmental Engineering,
Via G. Duranti 93, 06125 Perugia, Italy
{filippo.ubertini,nicola.cavalagli,alban.kita}@unipg.it

[3] University of Minho
Department of Civil Engineering,
Campus de Azurém, 4800-058 Guimarães, Portugal
{lramos,mgm}@civil.uminho.pt

Keywords: Historical masonry structure, Structural Health Monitoring, Seismic induced damages, Environmental effects, Operational Modal Analysis, Sonic Test.

Abstract. *The San Pietro bell tower belongs to a monumental complex of exceptional historical, cultural and artistic value and is considered one of the landmarks of Perugia, Italy. The preservation of this structure has been considered an essential issue over centuries and even more nowadays. For this reason, a permanent vibration-based Structural Health Monitoring (SHM) system able to detect anomalies in the structural behavior by means of statistical process control tools has been installed in the tower. The SHM system is based on the continuous identification of the natural frequencies of the bell tower and on the statistical analysis of their variations. Environmental parameters, i.e. temperature and humidity, are monitored as well for compensation purposes. The aim of this paper is to present the results of the most recent investigations carried out on the monument after the 2016-2017 Central Italy earthquake sequence whose effects were perceived also in Perugia, in spite of the significant distance from the epicenter of the main shocks (about 70 km). In particular, ambient vibration test and sonic tests were performed. Moreover, the dependence of the dynamic parameters on the environmental factors is studied by means of AutoRegressive output with an eXogenous input (ARX) models. The comparison of results in pre- and post-earthquake conditions allows detecting the modifications in the structural behavior of the tower.*

1 INTRODUCTION

Historical masonry constructions are susceptible to damages related to the effects of soil settlements, weathering, human actions, deformations, material degradation and exceptional events. In particular, in seismic countries like Italy, the vulnerability of cultural heritage against earthquakes is one of the major concern. The maintenance and conservation are an expensive duty for the owner and the availability of automated methods for damage assessment is definitely attractive. The aim of Structural Health Monitoring (SHM) is to provide, on a continuous basis, a diagnosis of the state of a structure, at both local and global levels. The possibility of recording and processing data over time allows to detect damages at very early stage as well as to provide a prognosis about their evolution. Moreover, SHM techniques permit a condition-based maintenance instead of scheduled or breakdown operations. As global methods, SHM systems are able to alert about the occurrence of damage and, in some cases, to localize it, but they generally fail at providing detailed information about the extent and the type of such a damage. Other types of complementary investigations are therefore necessary to pinpoint the damage and characterize it. Despite that, SHM is always indicated in case of cultural heritage, where the need of minimum intervention often limits the range of applicable techniques for structural characterization [1].

The focus of this paper is on the San Pietro bell tower in Perugia, Italy. It is part of San Pietro complex, which includes the basilica, three cloisters, the bell tower and several buildings that embody the monastery, the Department of Agriculture of University of Perugia, and the seismic observatory "Andrea Bina". Starting from 2013, the bell tower has been object of dynamic investigations and numerical modeling by a team of researchers from the Department of Civil and Environmental Engineering of University of Perugia. The purpose of these studies was the installation of a permanent vibration-based SHM system able to detect anomalies in the structural behavior by means of statistical process control tools such as control charts. The system was activated in December 2014. The SHM is based on the continuous identification of the natural frequencies of the bell tower and on the analysis of their variations. The fluctuations are associated to the daily and seasonal variations of environmental parameters and freezing conditions. By chance, exceptional events were also observed, namely the series of violent earthquakes that hit Central Italy in the period August 24th, 2016 - January 18th 2017, that caused some slight structural damage clearly detected by the SHM system [2]. Their effects were perceived also in Perugia, even if only minor damages occurred.

The most recent investigations carried out on the monument are presented in this paper. The starting point of the work was the collection of information about the structure, namely historic analysis and literature review. Indeed, any investigation on historic structures depends on the accurate knowledge of this information. In situ investigations were carried out in May 2017 with the aim of corroborating the available information and gathering new one. The new study included (1) visual survey, (2) Sonic Tests (STs), and (3) Ambient Vibration Tests (AVTs). The results of STs were used to characterize the materials of the tower, whereas the results of AVTs were used to detect possible changes in the dynamic properties of the tower following the 2016-2017 earthquakes as well as to better characterize its mode shapes (a higher number of sensors was deployed with respect to previous testing campaigns). Moreover, data from continuous monitoring were analyzed, i.e. natural frequencies and environmental parameters. Based on the correlation analysis, the dynamic response of the monument was modelled by means of ARX models.

2 CASE STUDY: SAN PIETRO BELL TOWER

2.1 Historic analysis

Extensive studies were conducted in various historical archives of Perugia [3]. The abbey was erected in the year 996 on the former Episcopal Church of the city. The first historical evidence about the bell tower is a document dating from 1286. Substantial modifications in the structure were carried out at the end of the 14th century. In 1387, the cusp and part of the belfry were demolished in order to transform the bell tower into a defensive tower and the monastery into a fortress. The reconstruction of the steeple began in 1463. The project was commissioned to the architect Bernardo Gambarelli, called Rossellino, to whom the actual aspect of the bell tower is attributed (Figure 1). During the centuries, the bell tower has undergone numerous repair interventions following damages caused by earthquakes and, especially, lightnings. The chronicles refer to collapses and damages caused by lightnings and consequent restoration works in the years 1481, 1498, 1569, 1574, 1592, 1616, 1618, 1640, 1667, 1674, 1730, 1778, and 1787. In 1788 one of the earliest modern protective lightning rod was installed on the tower.

In the last century, three large structural interventions were carried out on the monument. Between 1929 and 1933, a metal frame supporting the four bells was built. The intervention was considered necessary to reduce the oscillations caused by the ringing of the bells. However, it turned out to be rather invasive. In fact, the metal frame is directly supported by the walls of the shaft, penetrating their entire thickness. It is 9 m high, and its weight is about 5500 kg. In 1951, some consolidation works were carried out by the well-known engineer Sisto Mastrodicasa. In 1997 the monument underwent various damages as a consequence of the Marche-Umbria earthquake. They were repaired in 2002 [4]. Carbon and glass fibers impregnated with epoxy resin and FRP bars were massively used to strengthen the cusp and the belfry.

Figure 1: Ancient representations of the bell tower: a) Register of Collegio del Cambio, by Matteo di Ser Cambio, 1377; b) fresco in Priori Palace, by Benedetto Bonfigli, 1455-1479; c) painting of Perugia, by Gaspar Van Vittel, early 18th century.

2.2 Geometrical and material surveys

The tower is 61.45 m high and can be subdivided in four main parts, namely (1) basement; (2) shaft; (3) belfry; and (4) cusp, see Figure 2. The basement has a truncated dodecagonal pyramid shape and a height of 8 m. It is characterized by massive stone walls, with thickness ranging roughly from 2 m to 3.5 m. Inside, the basement consists of a semispherical dome of 6 m diameter. The external leaves of the basement are made of irregular travertine blocks. The shaft rests on the basement, at a height of 4.5 m from the ground, has a dodecagonal cross section and reaches a height of 27 m. The average thickness of the walls is 1.8 m. The outer leaf is made of limestone blocks and brick insertions. Inside, the structure is particularly complex, but it can be subdivided into two spaces. The lower room consists of a second hemispherical vault. The second room is located at a height of 11.6 m and occupies the remaining volume of the shaft. Here, the metal structure supporting the bells rises. The materials used for the internal structure are strongly inhomogeneous. The walls are mostly made of limestone masonry, while arches and vaults are made of bricks. Some concrete elements are present as well. A concrete floor separates the shaft from the belfry. The belfry has a hexagonal shape and rises up to a height of 41 m. The thickness of the walls decreases to 1.2 m. The lower part of the belfry is pierced by six openings. Likewise, large mullioned windows characterize the upper part. Here, the materials are travertine and brick masonry. The cusp completes the bell tower on top, reaching a total height of 61.5 m. It has the shape of a hexagonal pyramid and thickness of 1 m. Concerning the materials, the last 6 m are composed by a solid masonry block, featuring a cusp mainly made of travertine with an external brick layer.

Figure 2: San Pietro bell tower: a) North-West side of the tower; b) Basement; c) Interior of the tower; d) Metal structure supporting the bells; e) One of the mullioned window; f) Interior of the cusp.

2.3 Continuous Structural Health Monitoring

The continuous dynamic monitoring of the bell tower started on December 9th, 2014 [2]. The monitoring system is composed of several components: sensors, data acquisition system, data communication system, data processing system, and data storage system. Three uniaxial piezoelectric accelerometers, model PCB 393B12, with a sensitivity of 10V/g, together with the data acquisition system are located at the base of the cusp. Data are acquired using a multi-channel system, carrier model cDAQ-9184, with NI 9234 data acquisition modules and a sampling frequency of 100 Hz. The acquisition system is connected to a host personal computer (PC) placed in the shaft, below the belfry. A LabVIEW code, implemented in the PC, is used for data acquisition and real time elaboration, such as amplitude and spectral plots. The data provided by the accelerometers are recorded at about 1600Hz, down-sampled at 100 Hz, and stored in distinct files of 30 recording minutes for automated modal identification. From the computer, the data are sent via internet to a remote server located in the Laboratory of Structural Dynamics of the Department of Civil and Environmental Engineering of University of Perugia, where they are processed through a specific MatLab code. Since March 2015, environmental sensors are placed, in both the cusp and the belfry, including two thermocouples connected to the cDAQ-9184, which measure the temperature every 30 minutes. Standalone sensors, model Tinytag from Gemini Data Loggers, consisting of eight temperature sensors (six dry bulb sensors and two surface sensors) and two humidity sensors are also installed. They acquire and register by themselves environmental data every 30 minutes. A summary of the environmental sensors installed on the bell tower is provided in Table 1.

The SHM is based on the continuous identification of the natural frequencies of the bell tower and on the analysis of their variations. Any changes in the dynamic behavior of the structure are automatically detected by means of statistical process control tools of the identified modal frequencies using automated OMA techniques. The procedure involves the following steps: (1) automated modal identification and modal tracking processes, (2) removal of environmental effects, and (3) damage detection. The first step includes: (1) a pre-processing analysis to identify and correct anomalies in the data, (2) detection and removal of vibrational data under the action of the swinging bells, (3) application of a low-pass filter and decimation of data to 40 Hz, (4) application of a fully automated stochastic subspace identification (SSI) procedure [5], and (5) modal tracking of the estimated parameters based on a similarity check. Then, a combination between the techniques of multivariate linear regression (MLR) and principal component analysis (PCA) is adopted to remove the environmental effects. Finally, the novelty analysis procedure is used for damage detection.

Sensor n.	Variable name	Measurement type	Location	Height [m]	Orientation
1	T_1	Air temperature	Shaft indoor	12	S
2	T_2	Surface temperature	Shaft outdoor	24	S
3	T_3	Surface temperature	Shaft indoor	24	S
4	T_4	Air temperature	Shaft indoor	24	N
5	T_5	Air temperature	Belfry outdoor	27	S
6	T_6	Air temperature	Befry outdoor	27	N
7	T_7	Air temperature	Cusp indoor	41	S
8	T_8	Air temperature	Cusp indoor	41	N
9	φ_1	Air humidity	Shaft indoor	12	S
10	φ_2	Air humidity	Belfry outdoor	27	S

Table 1: Environmental monitoring sensors installed on the bell tower.

3 INSPECTION AND TESTING

In May 2017, new studies were conducted on the San Pietro bell tower by the authors of this paper. They consisted of (1) visual inspection and survey of the metal structure supporting the bells, (2) STs, and (3) AVTs. The methodology used in the investigations as well as the obtained results are discussed in this section.

3.1 Visual survey

The visual survey allowed verifying the information collected about the monument and constituted the first step of the in-situ investigations [6]. All sections of the bell tower were inspected (base, shaft, belfry and cusp). Special attention was devoted to the metal structure supporting the bells, as no previous survey was available. Indeed, the metal structure has been neglected in the previous studies on the bell towers. Furthermore, possible damages caused by the last earthquake were investigated [2].

Globally, the bell tower appears to be in good state of conservation from the structural point of view. Major damages due to the last earthquakes are not clearly recognizable. Nevertheless, some thin cracks can be found in the lower portion of the belfry, in correspondence to the masonry arches above the lower windows, as shown in Figure 3, that are consistent with the diffused damaging expected from numerical simulations [2]. The good seismic behavior may be attributed to the extensive insertions of FRP materials executed during the last restoration works [4].

Figure 3: Cracks in the lower part of the belfry.

3.2 Sonic test

Sonic Pulse Velocity Test is a NDT method based on the generation of a mechanical pulse in the sonic frequency range by percussion (hammer) and its collection through a receiver (unidirectional accelerometer) which can be located in different positions (direct, semi-direct or indirect tests). The difference between emitted and received signals can provide information about the medium it went through. Among the several parameters that characterize waves (i.e. velocity, energy and wavelength), velocity is the property most often used in sonic testing. This parameter can be determined once the travel time and distance between transmitter and receiver are known. Afterwards, velocities can be correlated with the compressive strength and the elastic properties of masonry [7]. In case of homogeneous materials, analytical relations exist between the velocity V of elastic waves, the Young's modulus E, the Poisson's ration υ, and the density ρ:

$$V_p = \sqrt{\frac{E(1-\upsilon)}{\rho(1+\upsilon)(1-2\upsilon)}} \qquad V_r = \frac{0.87+1.12\upsilon}{1+\upsilon}\sqrt{\frac{E}{\rho}\frac{1}{(1-2\upsilon)}} \tag{1}$$

where V_p and V_r are the velocities of elastic compression waves P and surface Rayleigh waves R, respectively. The former can be measured by means of direct STs, whereas the latter using indirect tests [8].

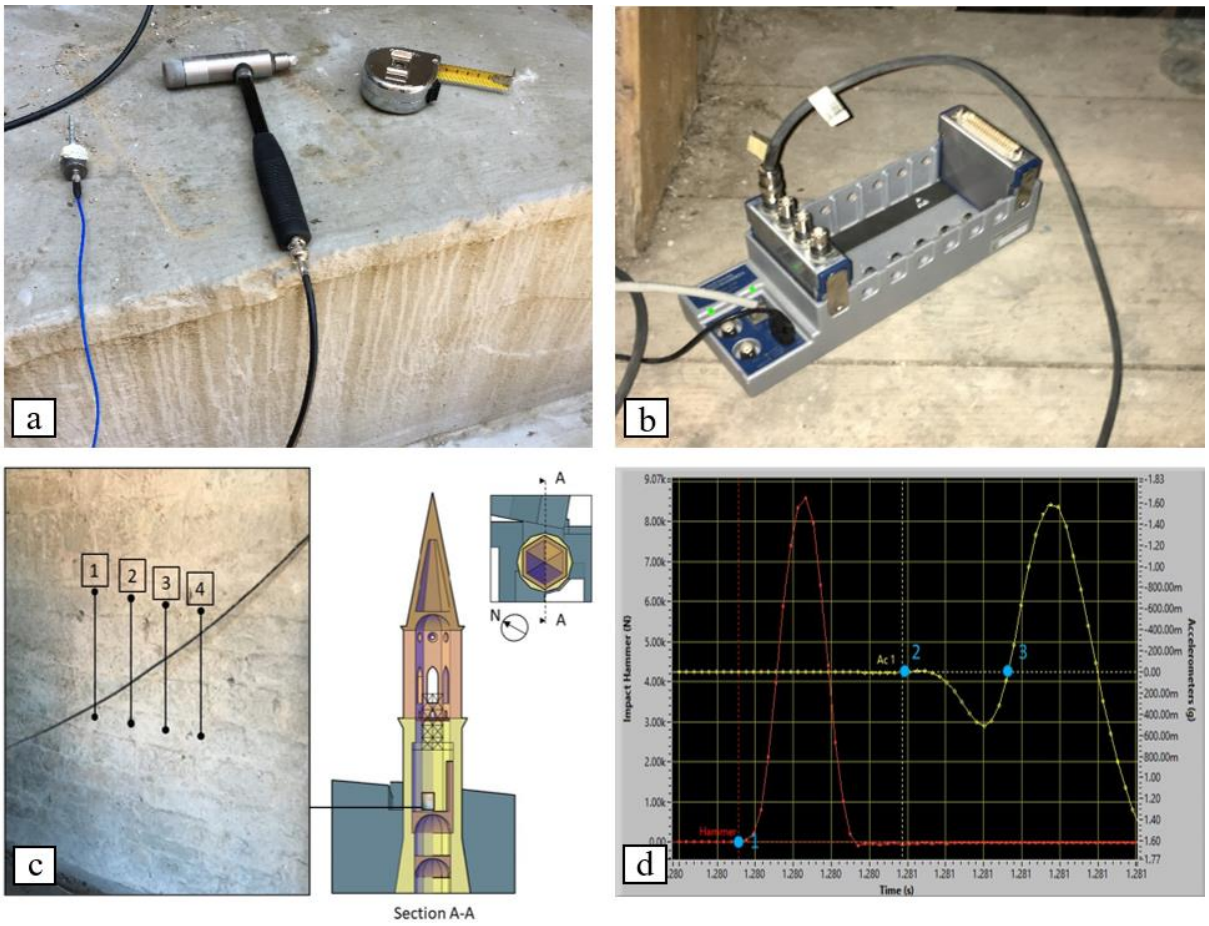

Figure 4: a) Equipment for ST: uniaxial accelerometer, hammer, ruler; b) Acquisition system; c) Example of indirect test configuration (interior stone masonry); d) Typical output from a ST: the red curve corresponds to the signal of the hammer and the yellow one to the signal recorded by the accelerometer; Point 1: impact of the hammer; Point 2: P-wave arrival; Point 3: R-wave arrival.

As for the present case study, both indirect and direct STs were conducted to characterize materials, see Figure 4. The indirect STs allow characterizing only the exterior layers of the wall. Thus, the investigation was integrated with direct STs, which provide additional information about the inner portion of the wall. The indirect tests were carried out on the shaft in correspondence of: (1) interior stone masonry; (2) interior brick masonry; (3) exterior stone masonry; (4) exterior brick masonry. The tests were performed in three or four points, roughly 20 cm apart. The distance assumed between accelerometer and impact area of the hammer are 0.6 m and 1 m. The direct tests were conducted in proximity of the entrance door and the window of the shaft, where both sides of the wall could be easily accessed. The adopted equipment consisted in hammer, accelerometer, DAQ system, personal computer, and coaxial cables. Data were acquired with a sampling frequency of 50,000 Hz. Ad hoc developed Labview toolkits were used to acquire and analyze data. ST results are summarized in Table

2. The measured wave velocities in indirect and direct tests are comparable. This indicates that the inner material of the three-leaf masonry of the shaft presents high density and therefore good mechanical properties. The high values of wave velocity found in the masonry close to the window may be explained by the presence of bigger size stones in proximity of the opening. The obtained values of wave velocities are then used to estimate the dynamic Young's modulus of the masonry material by means of Equations 1. The results, summarized in Table 3, confirm to some extent the quite large static Young's modulus of the shaft that was estimated in previous works on the bell tower by calibration of numerical models, namely 5520 MPa [9], 5450 MPa [10] and 5678 MPa [11]. The challenge in STs is then relating the dynamic modulus to the static one. More extensive experimental campaigns would be needed to compute the ratio between dynamic and static modulus of masonry materials.

	Mean velocities [m/s]		Coefficient of variation [%]	
	Vp	Vr	CVp	CVr
Indirect Test				
Interior stone masonry – 0.60 m	2818	1381	9	7
Interior stone masonry – 1.00 m	3378	1375	7	4
Interior brick masonry – 0.60 m	1378	550	13	11
Exterior stone masonry – 0.60 m	2203	1197	6	12
Exterior stone masonry – 1.00 m	3079	1203	10	12
Exterior brick masonry	1219	571	14	22
Direct Test				
Shaft - Window	2882	/	3	/
Shaft - Door	2306	/	10	/

Table 2: ST results: wave velocities.

	ρ [kg/m3]	E_d [GPa]
Interior stone masonry – 0.60 m	2200	12.68
Interior stone masonry – 1.00 m	2200	12.68
Interior brick masonry	1800	1.67
Exterior stone masonry – 0.60 m	2200	9.29
Exterior stone masonry – 1.00 m	2200	9.78
Exterior brick masonry	1800	1.78

Table 3: Estimated values of dynamic Young's moduli.

3.3 Experimental dynamic identification

On May 18th, 2017 a new AVT was carried out on San Pietro bell tower. The objective was to detect any possible changes in the dynamic properties of the tower following the 2016-2017 earthquakes as well as to better characterize the mode shapes of the structure by means of a higher number of sensors. Twelve uniaxial piezoelectric accelerometers, model PCB 393B12, were used in total. They were placed at four levels, at the height of 21 m, 24 m, 27 m, and 41 m, see Figure 5. At each level, three sensors were positioned, along the directions X, -Y and Y. The additional accelerometer in Y direction was necessary to detect torsional modes. Data were acquired using a multi-channel system, carrier model cDAQ-9188, with NI 9234 data acquisition modules. Accelerations were recorded for two hours and a half and processed with ARTeMIS software (version 5.0) in which several Operational Modal Analysis (OMA) techniques are available. In this study, the Enhanced Frequency Domain Decomposition (EFDD) and the Stochastic Subspace Identification – Principal Components

(SSI-PC) are used. The results (natural frequencies, damping ratios and mode shapes) are considered cross-validated when the same modes are identified by both identification techniques.

Six vibration modes are found: the first two bending modes in X and Y direction f_{x1} and f_{y1}, the third torsional mode f_{t1}, the second mode in Y direction, and the other two modes in X direction f_{x2} and f_{x3}, see Figure 6 and Table 4. The mode shapes obtained with the two different identification techniques appear quite consistent since the Modal Assurance Criterion (MAC) values are close to the unity, see Table 5.

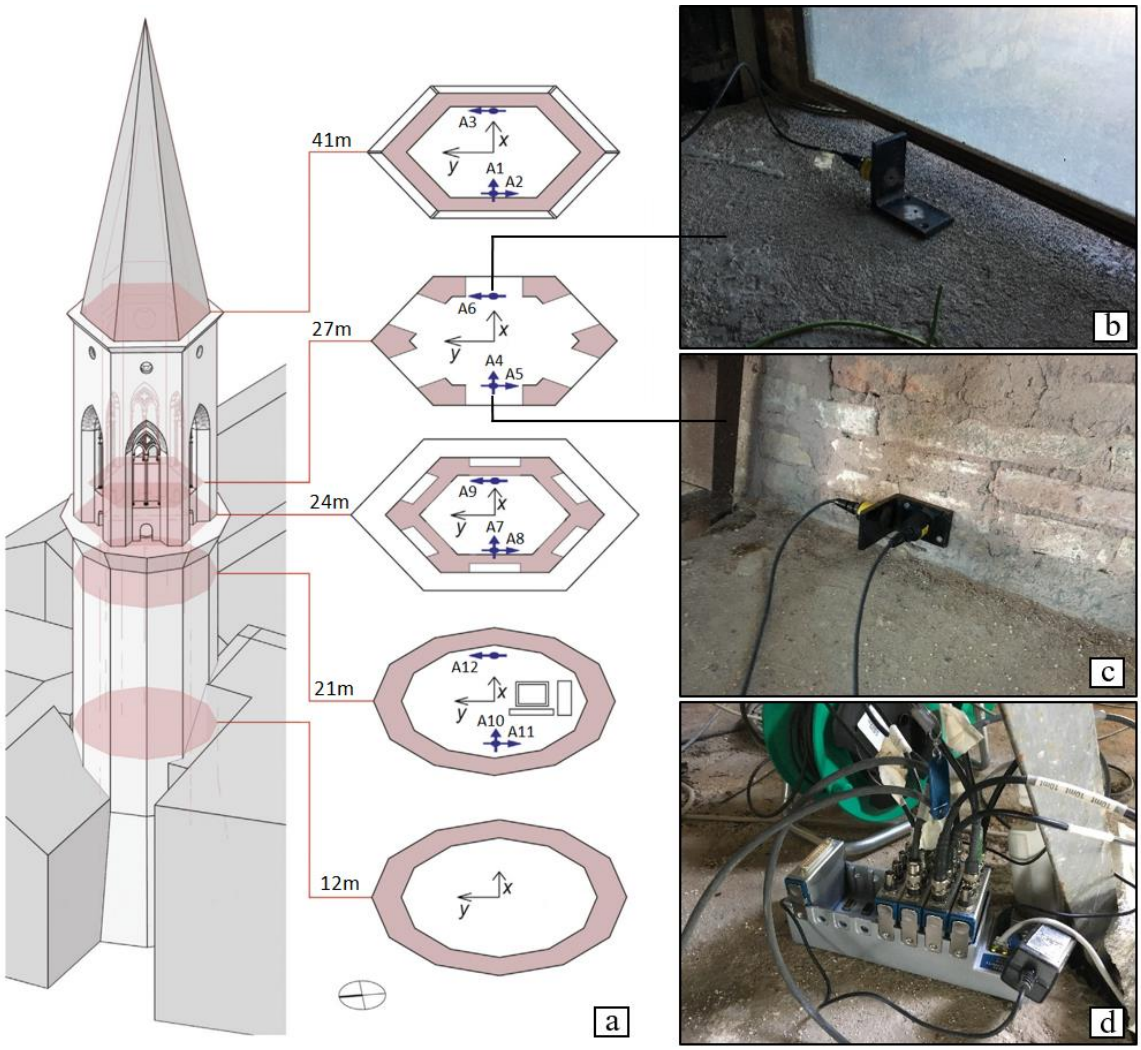

Figure 5: AVT: a) Localization of uniaxial accelerometers in the tower; b) Accelerometer in Y-direction c) Accelerometers in X- and Y-direction; d) Data acquisition system and cables.

The same methodology is applied to analyze experimental data acquired on February 2015, in pre-earthquake conditions. The AVT was carried out using six uniaxial piezometric accelerometers placed at two levels (24 m and 41 m). At each level, three sensors were positioned along the directions X, -Y and Y respectively. Data belonging to a different time window was used with respect to the one used in previous works [12]. Four modes are identified: the first two bending modes f_{x1} and f_{y1}, the torsional mode f_{t1}, and the other mode in X direction f_{x2}. Natural frequencies and relative damping ratios are listed in Table 6, while the MAC values computed between mode shapes are presented in Table 7. The identified mode shapes are shown in Figure 7. Once again, the mode shape configurations obtained from

both identification techniques appear quite similar, reading MAC values very close to the unity. Notwithstanding the consistency of the results, it was not possible to identify all the seven modes found in previous studies. In particular, the third mode in X direction f_{x3}, and the other modes in Y direction were not identified. The reason is likely due to the different time window (excitation conditions) used for the test and to the different dynamic identification techniques.

A comparison in terms of frequencies and MAC coefficients between the results obtained from the two AVTs are shown in Table 8. As far as frequencies are concerned, the first two bending modes do not present significant changes. On the contrary, the torsional mode and the second mode in X direction exhibit more significant modifications, which may be caused either by the occurrence of damages or by the effects of environmental factors. The MAC coefficients highlight substantial variation in the modal shapes of higher modes in post-earthquake conditions.

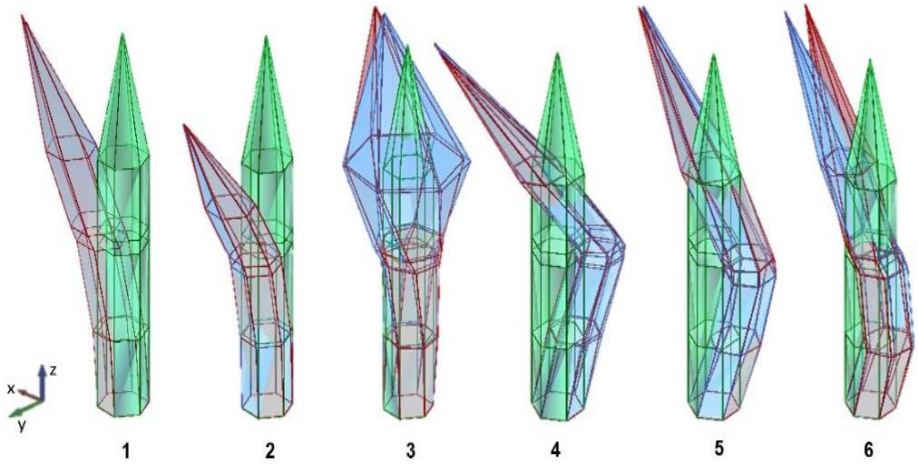

Figure 6: Identified mode shapes: undeformed structure in green, EFDD estimator in red, SSI-PC estimator in blue.

Mode number	EFDD		SSI-PC		Mode Type
	f [Hz]	ξ [%]	f [Hz]	ξ [%]	
1	1.460	1.185	1.458	0.802	f_{x1}
2	1.526	0.488	1.526	0.730	f_{y1}
3	4.169	0.942	4.176	1.141	t_1
4	4.500	0.430	4.487	0.923	f_{y2}
5	4.972	1.219	4.983	2.218	f_{x2}
6	7.252	0.056	7.116	2.223	f_{x3}

Table 4: AVT results: frequencies and relative damping.

	EFDD [Hz]	1.460	1.526	4.169	4.500	4.972	7.252
SSI-PC [Hz]	1.458	**0.999**	0.003	0.011	0.007	0.009	0.352
	1.526	0.004	**0.991**	0.005	0.014	0.000	0.007
	4.176	0.012	0.008	**0.944**	0.016	0.032	0.097
	4.487	0.007	0.016	0.063	**0.929**	0.461	0.336
	4.983	0.008	0.001	0.082	0.539	**0.993**	0.507
	7.116	0.326	0.045	0.165	0.285	0.444	**0.920**

Table 5: Scalar MAC between mode shapes.

Mode number	EFDD		SSI-PC		Mode Type
	f [Hz]	ξ [%]	f [Hz]	ξ [%]	
1	1.458	1.131	1.455	1.014	f_{x1}
2	1.526	0.774	1.525	1.113	f_{y1}
3	4.357	1.217	4.376	2.560	f_{t1}
4	4.617	0.171	4.620	3.136	f_{x2}

Table 6: AVT results in pre-earthquake conditions: frequencies and relative damping.

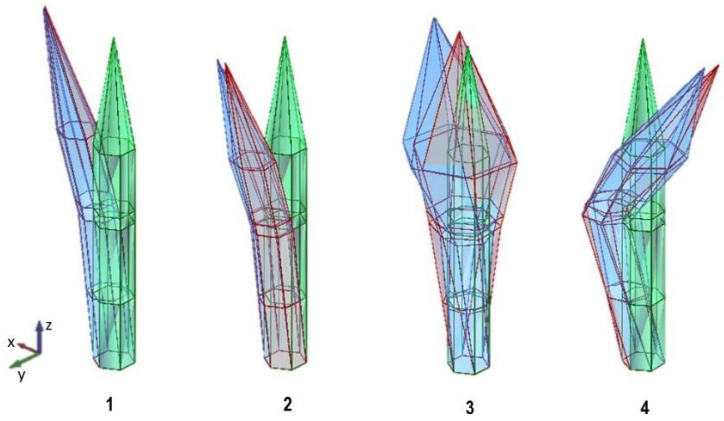

Figure 7: Identified mode shapes in pre-earthquake condition: undeformed structure in green, EFDD estimator in red, SSI-PC estimator in blue.

	EFDD	1.458 [Hz]	1.526 [Hz]	4.357 [Hz]	4.617 [Hz]
SSI-PC	1.455 [Hz]	**0.999**	0.013	0.082	0.065
	1.525 [Hz]	0.003	**0.982**	0.002	0.052
	4.376 [Hz]	0.035	0.010	**0.979**	0.355
	4.620 [Hz]	0.035	0.010	0.025	**0.921**

Table 7: Scalar MAC between mode shapes in pre-earthquake conditions.

Mode type	f [Hz] - EFDD		Δf (%)	MAC	f [Hz] – SSI-PC		Δf (%)	MAC
	AVT2	AVT3			AVT2	AVT3		
f_{x1}	1.458	1.460	+0.14	0.978	1.455	1.458	+0.21	0.987
f_{y1}	1.526	1.526	<0.01	0.969	1.525	1.526	+0.07	0.979
f_{t1}	4.357	4.169	-4.31	0.908	4.376	4.176	-4.57	0.738
f_{y2}	/	4.500	/	/	/	4.487	/	/
f_{x2}	4.617	4.972	+7.69	0.694	4.620	4.983	+7.86	0.818
f_{x3}	/	7.252	/	/	/	7.116	/	/

Table 8: Results comparison by means of MAC values.

4 LONG-TERM MONITORING ANALYSIS

The long-term monitoring data concern natural frequencies, air and surface temperatures, and air humidity. Five modes are continuously tracked in operational conditions by means of a fully automated SSI technique: the first two bending modes f_{x1} and f_{y1}, the third torsional mode f_{t1} and the other two modes in the Y direction, f_{y2} and f_{y3}. Data related to frequencies are available since December 2014 while environmental data are available since March 2015. The plot of the identified frequencies over time is presented in Figure 8. The reader is referred to [12] for an exhaustive analysis of hygrothermal effects on natural frequencies. In this paper, sensors T_2, T_3, T_5, T_7, T_8, H_5 are taken into account. Long-term records are subdivided

in three sets for the analysis. Data collected in the period March 2nd, 2015-August 23rd, 2016 belong to the first set and are related to pre-earthquake conditions. Data collected between January 19th and December 31th, 2017 belong to the second set and are considered related to post-earthquake conditions. Data recorded between the afore-mentioned periods are not analyzed since seismic events were occurring. Following, the correlations between environmental data and frequencies are studied in pre- and post- earthquake conditions. Furthermore, the dependence of the dynamic parameters on the environmental factors is studied by means of AutoRegressive output with an eXogenous input (ARX) models.

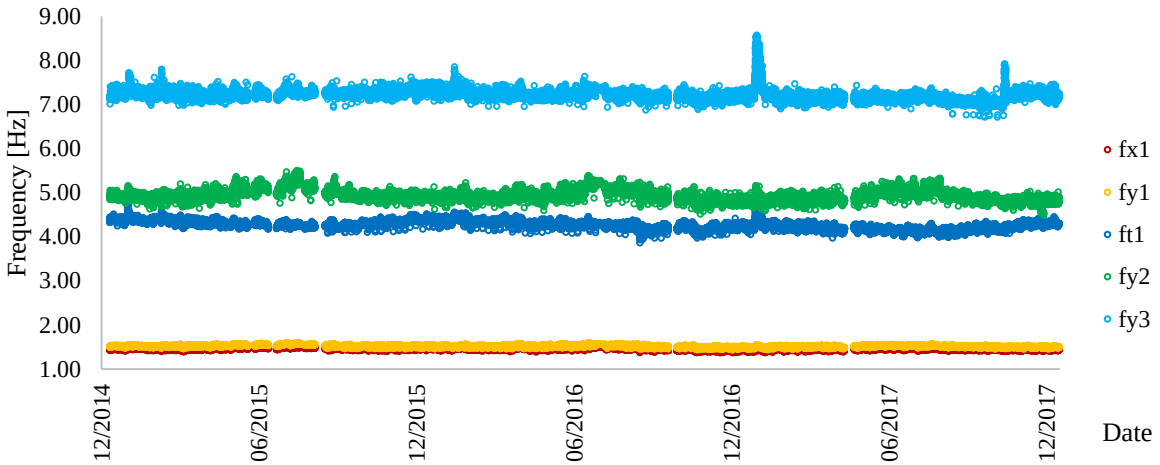

Figure 8: Identified natural frequencies over time.

4.1 Correlation analysis

Correlation coefficient between monitoring quantities in pre- and post-earthquake conditions are shown in Table 9 and Table 10, respectively. The frequencies of the first flexural modes exhibit positive correlation with temperature data sets. An increase in temperature determines an increase in natural frequencies. These results are in accordance with other literature studies and they can be explained with the closing of micro-cracks within mortar layers as a result of the thermal expansion of the material [13]. For the sake of clarity, a comparison between the time history plots of temperature T_5 and frequency f_{x1} is shown in Figure 9 as an example. It can be easily noticed that the two variables have the same trend in time. The plots showing the correlation between natural frequencies and temperature are provided in Figure 10 and Figure 11. Frequency-temperature relations are almost linear, with equation:

$$f_i = f_{i,0} + \kappa_{i,T} Tsi \tag{2}$$

where $\mathrm{i} = \mathrm{x1}, \mathrm{x2}, \mathrm{T}, \mathrm{y2}, \mathrm{y3}$ indicated the mode, si the number of the temperature sensors presenting the highest correlation with the mode i, $f_{i,0}$ is the frequency at 0°C and $\kappa_{i,T}$ are the frequency–temperature sensitivity coefficients. The least square estimates are shown in Table 11 and Table 12. A comparison between the average frequencies before and after the earthquakes is reported in Table 13. Confidence limits are fixed multiplying the standard deviations by the factor 1.96, found in statistical t-distribution tables. In general, the average frequencies decrease after the seismic events. However, the values do not exceed the fixed confidence interval meaning that major damages did not occur. It is worth noticing that the torsional mode f_{t1} shows the major decrease in terms of average frequency value and the correlation between mode f_{y3} and the different temperature sets becomes strictly negative. The

results may indicate a stronger dependency between modes f_{t1} and f_{y3} and the behavior of the fiber reinforcements which are widely present in the belfry. The negative correlation is attributed to the thermally induced loss of tension in fiber reinforcements and tie elements mounted during the 2002 strengthening works [12]. Indeed, the two modes are the ones that imply the larger deformations in the belfry. The results of the correlation analysis are consistent with the damage pattern observed in the belfry during the visual inspection.

	T_2	T_3	T_5	T_7	T_8	H_5	f_{x1}	f_{y1}	f_{t1}	f_{y2}	f_{y3}
T_2	1	0.825	0.878	0.778	0.792	-0.763	0.667	0.722	-0.402	0.697	**0.135**
T_3		1	0.984	0.988	0.993	-0.697	0.619	0.719	-0.662	0.751	-0.015
T_5			1	0.957	0.968	-0.731	**0.700**	**0.782**	-0.552	**0.768**	0.053
T_7				1	0.998	-0.655	0.462	0.568	**-0.740**	0.639	-0.089
T_8					1	-0.667	0.465	0.572	-0.739	0.645	-0.093
H_5						1	-0.427	-0.441	0.239	-0.478	-0.116
f_{x1}							1	0.969	0.086	0.818	0.400
f_{y1}								1	-0.042	0.874	0.344
f_{t1}									1	-0.193	0.526
f_{y2}										1	0.267
f_{y3}											1

Table 9: Correlation coefficients in pre-earthquake conditions.

	T_2	T_3	T_5	T_7	T_8	H_5	f_{x1}	f_{y1}	f_{t1}	f_{y2}	f_{y3}
T_2	1	0.813	0.895	0.727	0.726	-0.677	0.664	0.712	-0.516	0.685	-0.145
T_3		1	0.956	0.944	0.944	-0.506	0.606	0.700	-0.770	0.740	-0.287
T_5			1	0.875	0.875	-0.606	**0.672**	**0.758**	-0.717	**0.766**	-0.260
T_7				1	0.999	-0.465	0.515	0.615	**-0.821**	0.688	**-0.325**
T_8					1	-0.461	0.547	0.650	-0.815	0.717	-0.316
H_5						1	-0.468	-0.517	0.477	-0.540	0.128
f_{x1}							1	0.965	-0.059	0.802	0.147
f_{y1}								1	-0.206	0.868	0.085
f_{t1}									1	-0.385	0.544
f_{y2}										1	0.017
f_{y3}											1

Table 10: Correlation coefficients in post-earthquake conditions.

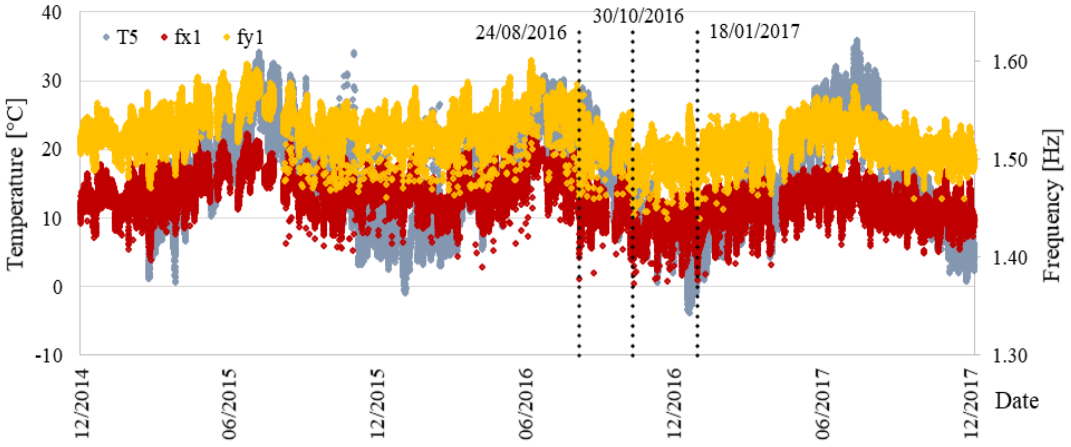

Figure 9: Time history plots of temperature T_5 and frequencies f_{x1} and f_{y1}.

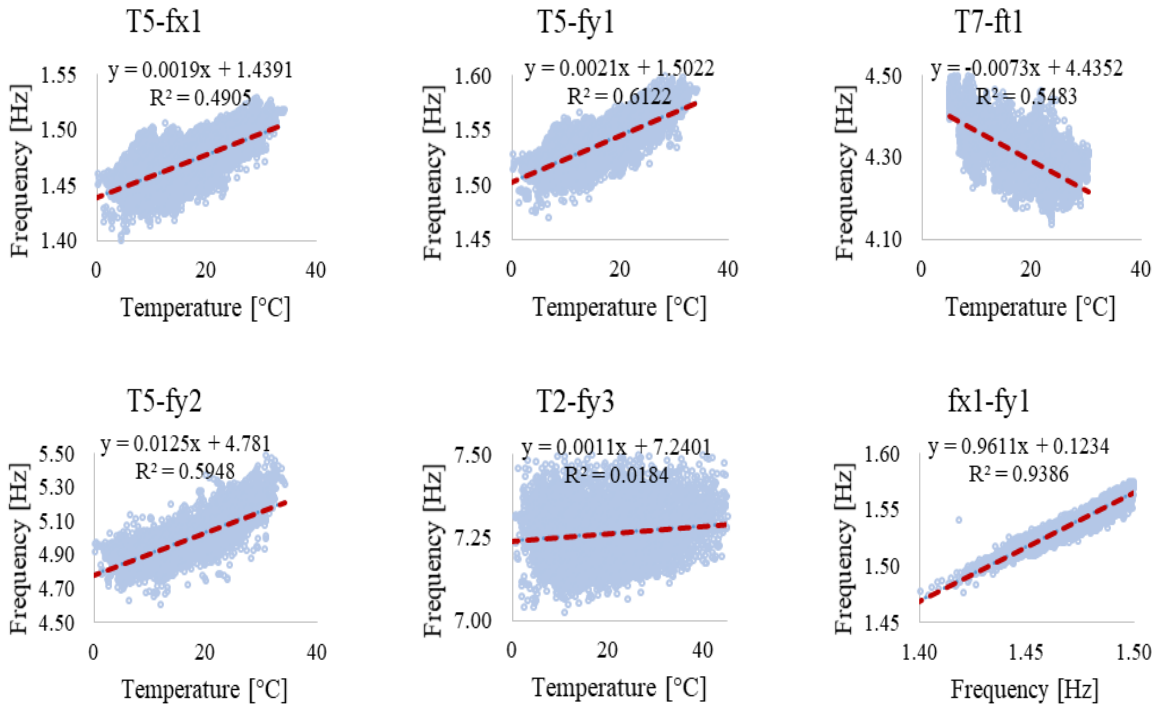

Figure 10: Plots of frequencies versus temperature data sets; plot between natural frequencies of modes f_{x1} and f_{y1} in pre-earthquake conditions; corresponding coefficients of determination.

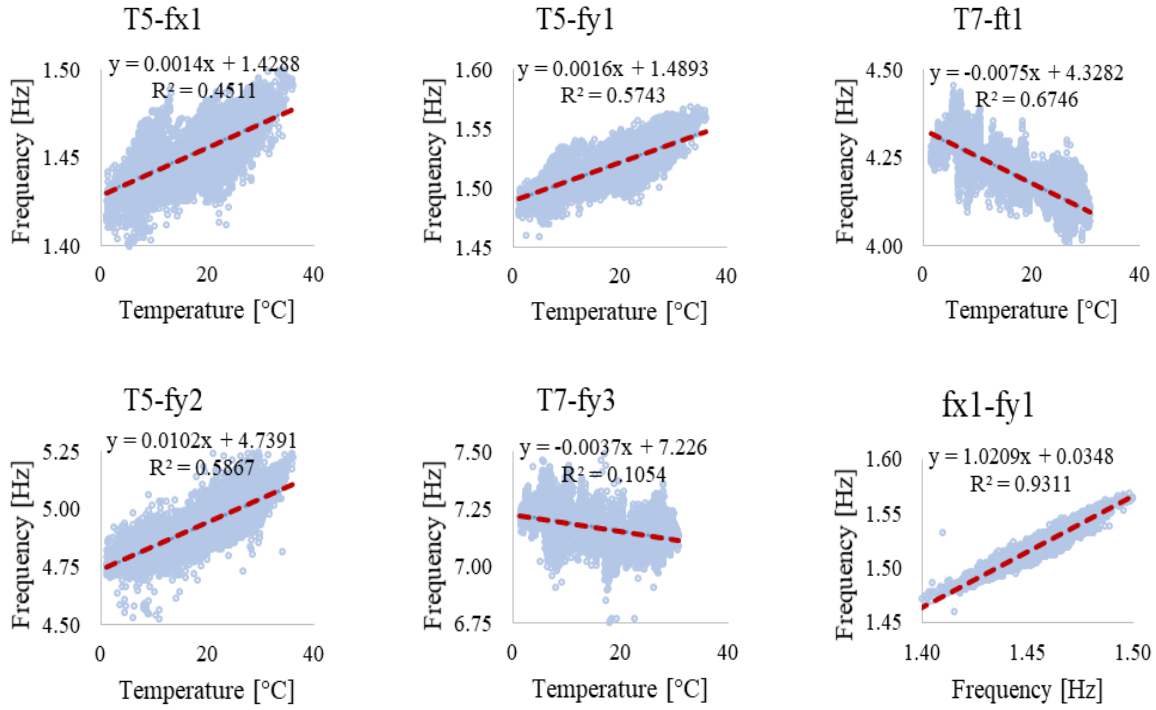

Figure 11: Plots of frequencies versus temperature data sets; plot between natural frequencies of modes f_{x1} and f_{y1} in post-earthquake conditions; corresponding coefficients of determination.

f_i	Tsi	$f_{i,0}$ [Hz]	$\kappa_{i,T}$ (mHz/°C)	R^2
f_{x1}	T_5	1.439	1.9	0.49
f_{y1}	T_5	1.502	2.1	0.61
f_{t1}	T_7	4.435	-7.3	0.55
f_{y2}	T_2	4.782	12.4	0.59
f_{y3}	T_5	7.240	1.1	0.02

Table 11: Parameters of best fitting lines between frequencies and temperature data in pre-earthquake conditions.

f_i	Tsi	$f_{i,0}$ [Hz]	$\kappa_{i,T}$ (mHz/°C)	R^2
f_{x1}	T_5	1.429	1.4	0.45
f_{y1}	T_5	1.489	1.6	0.57
f_{t1}	T_7	4.328	-7.5	0.67
f_{y2}	T_5	4.739	10.2	0.59
f_{y3}	T_7	7.226	-3.7	0.11

Table 12: Parameters of best fitting lines between frequencies and temperature data in post-earthquake conditions.

Mode	Average frequency [Hz]		Δf [%]	σ_f	Confidence interval [Hz]	
	Period 12/2014-08/2016	Period 01/2017-12/2017			Lower Bound	Upper Bound
f_{x1}	1.469	1.453	-1.085	0.019	1.431	1.506
f_{y1}	1.535	1.518	-1.113	0.019	1.497	1.572
f_{t1}	4.320	4.193	-2.961	0.063	4.195	4.443
f_{y2}	4.973	4.917	-1.119	0.112	4.750	5.192
f_{y3}	7.260	7.159	-1.388	0.074	7.111	7.406

Table 13: Comparison between natural frequencies in pre- and post- earthquake conditions.

4.2 ARX models

A common way to model the relation between environmental and modal parameters are linear, or multi-linear, regressions by means of the least squares method. All these models are referred to as static models because the response y in the instant k depends on the input u^{env} for the same instant. In other types of models, such as autoregressive models or dynamic models, the response depends also on previous inputs and outputs. These models are considered particularly suitable for representing the thermal inertia of the structure. [14]. One example of dynamic model is the AutoRegressive output with an eXogenous input (ARX) model:

$$\hat{y}_k + a_1 y_{k-1} + \cdots + a_{na} y_{k-na} = b_1 u^{env}_{k-nk} + b_2 u^{env}_{k-nk-1} + \cdots + b_{nb} u^{env}_{k-nk-nb+1} + e_k \qquad (4)$$

where a_i are the coefficients for the autoregressive part, b_i are the coefficients for the exogenous part, na and nb are the autoregressive and the exogenous orders, respectively, nk is the number of delays between input and output, and e_k is the unknown residual. Usually, the ARX model is defined according to the selected parameters na, nb and nk. The linear static model might be considered as an ARX model with parameters $na = 0, nb = 1, nk = 0$.

The frequency dependence of the first three modes on the environmental factors is studied by means of linear and ARX models in post-earthquake conditions. Several ARX model were tested changing the model parameters. Two types of input are considered: (1) the temperature showing the maximum correlation with the dynamic parameter; and (2) the six available

environmental data sets. The training period is 120 days. The average normalized prediction error was used as a quality criterion to assess the fit of the different models: The values obtained for both linear and ARX models are presented in Table 14. In general, it is observed that the two models provide similar results. The prediction error increases when considering only one input. Concerning the ARX-model based results, the plots of the identified and predicted natural frequencies are shown in Figure 12, Figure 15, and Figure 18. The corresponding residuals plots are displayed in Figure 13, Figure 16, and Figure 19. The plot of the experimental frequencies versus the simulated ones shows that the model is not able to follow the picks of temperatures, since the angular coefficient of the interpolation line is minor than one, see Figure 14, Figure 17, Figure 20. Note that all the results provided are relative to the ARX model with parameters $na = 1, nb = 3, nk = 1$.

Frequency	f_{x1}	f_{y1}	f_{t1}	f_{x1}	f_{y1}	f_{t1}
Input	T_5	T_5	T_7	T_2,T_3,T_5, T_7, T_8, H_5		
Linear model	0.0065	0.0061	0.0076	0.0045	0.0040	0.0066
ARX model	0.0066	0.0067	0.0071	0.0042	0.0037	0.0066

Table 14: Average normalized prediction errors.

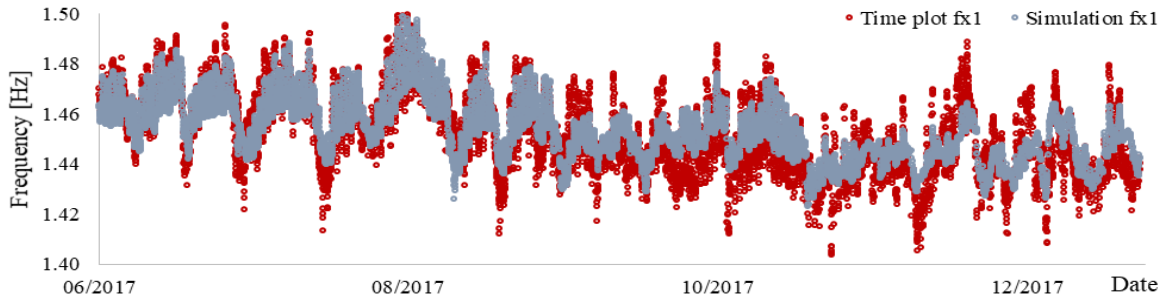

Figure 12: Time plot of identified and predicted frequency f_{x1}.

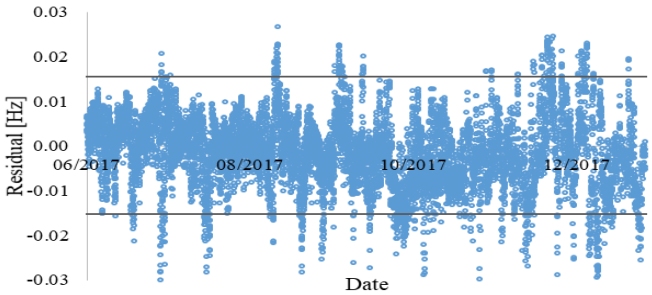

Figure 13: Plot of residuals between identified and predicted frequency f_{x1}.

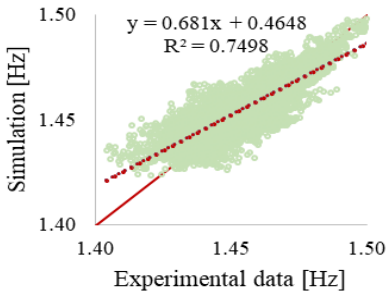

Figure 14: Experimental frequency f_{x1} versus the simulated one.

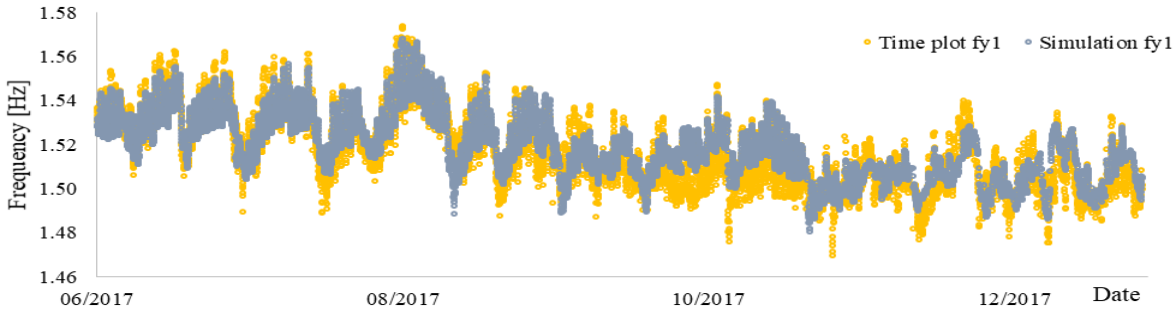

Figure 15: Time plot of identified and predicted frequency f_{y1}.

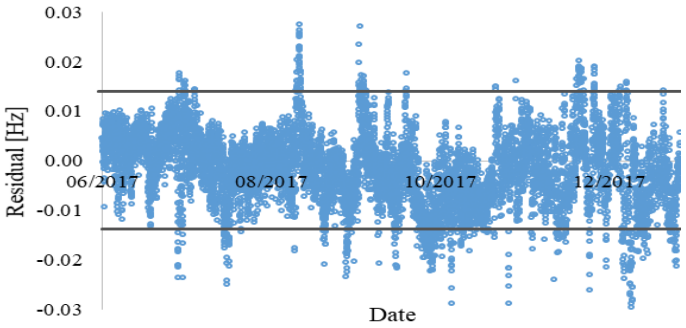

Figure 16: Plot of residuals between identified and predicted frequency f_{y1}.

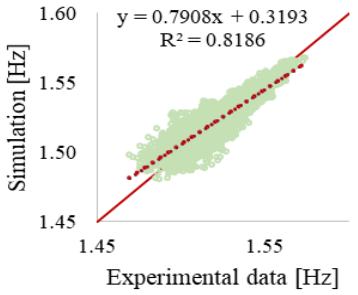

Figure 17: Experimental frequency f_{y1} versus the simulated one.

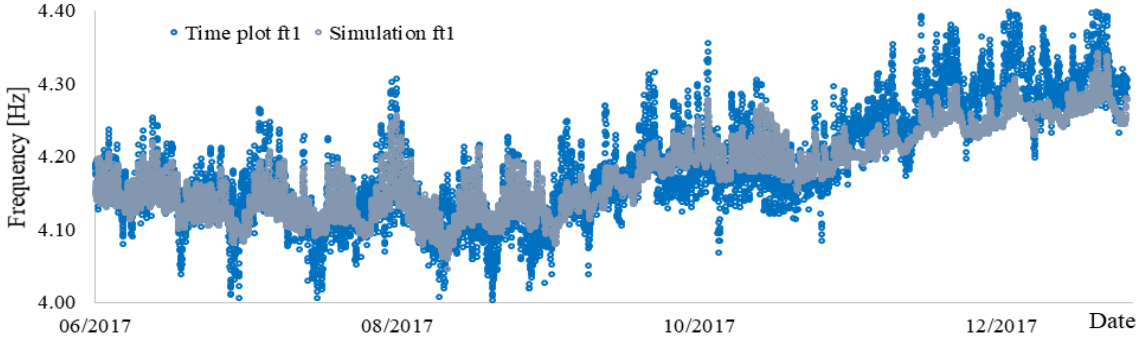

Figure 18: Time plot of identified and predicted frequency f_{t1}.

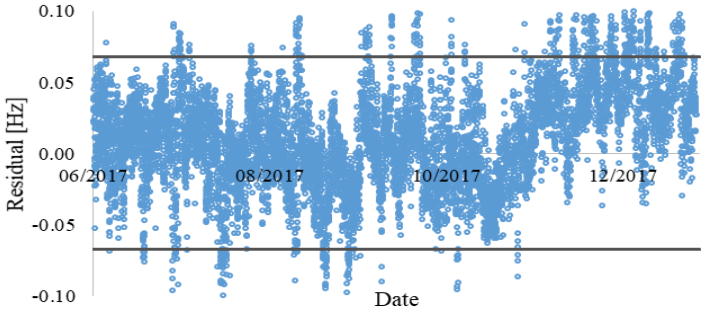

Figure 19: Plot of residuals between identified and predicted frequency f_{t1}.

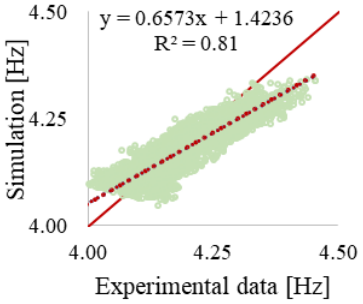

Figure 20: Experimental frequency f_{t1} versus the simulated one.

5 CONCLUSIONS

The most recent investigations carried out on the monumental San Pietro bell tower in Perugia, Italy, are presented in this paper. The main objective was to detect any change in the structural behavior following the 2016-2017 Central Italy earthquakes.

- The present aspect of the bell tower is the result of its complex history. It has been subject to numerous repair interventions over time following damages caused by earthquakes and, especially, lightnings. The structural works carried out in the years 1929-1933 have revealed to be particularly deleterious. More respectful restoration works were performed in 2002 after the 1997 Marche-Umbria earthquake. New techniques and modern materials were used to repair and consolidate the structure.
- Starting from 2013, several investigations have been carried out aiming at installing a permanent vibration-based structural health monitoring (SHM) system able to detect anomalies in the structural behavior by means of statistical process control tools. The

SHM is based on the continuous identification of the natural frequencies of the bell tower and on the analysis of their variations. Environmental parameters, i.e. temperature and humidity, are monitored as well. In particular, it is possible to track five modes among the seven identified.

- Concerning the visual survey, the monument appears in good state of conservation. However, some thin cracks are found in the lower portion of the belfry. The geometrical survey of the metal structure supporting the bells was carried out.
- Indirect and direct STs were performed to characterize materials. The investigated materials belong to the shaft of the tower: interior stone masonry, interior brick masonry, exterior stone masonry, exterior brick masonry. The direct tests were conducted in proximity of the entrance door and the window of the shaft, where both sides of the wall could be reached. The values of wave velocities are used to estimate the dynamic elastic moduli of masonry materials. The results support the Young's moduli estimated in previous works.
- Data from recent AVTs were analyzed. Six modes are found: the first two bending modes f_{x1} and f_{y1} and the third torsional mode f_{t1}, a second mode in Y direction, and two additional modes in the X direction (f_{x2} and f_{x3}). The results are compared with experimental data obtained in pre-earthquake conditions by means of MAC values. The torsional mode and the second mode in X direction exhibit significant alterations.
- Five frequencies are continuously tracked: f_{x1}, f_{y1}, f_{t1}, f_{y2}, and f_{y3}. The first three bending modes show clearly a positive correlation with temperature and a negative correlation with humidity. The torsional mode presents the opposite behavior. Frequency f_{y2} exhibits a strictly negative correlation with temperature only in post-earthquake conditions. The average frequencies decrease after the seismic events, according to what already observed in previous work. It is noted that modes f_{t1} and f_{y3} exhibit the major decrease in the average values of their natural frequencies. Indeed, the two modes are the ones that imply the larger deformations in the belfry. The results of the correlation analysis are consistent with structural damages in the belfry of the tower.
- ARX models are able to predict the natural frequencies of the structure with good approximation. However, the results are quite similar with those obtained with a linear model without delay. The accuracy of the prediction increases when the number of input in the models increases.

6 ACKNOWLEDGEMENTS

Most of the material presented in this paper belongs to the dissertation that the first author has carried out to obtain the master's degree in Structural Analysis of Monuments and Historical Constructions (SAHC) from the Polytechnic University of Catalonia (UPC), Spain, and the University of Minho (UMinho), Portugal. The SAHC Consortium is gratefully acknowledged for the scholarship provided to participate in the program. In addition, the Department of Civil and Environmental Engineering of University of Perugia is gratefully acknowledged for supporting the master's candidate and the hospitality in Umbria.

This project has received funding from the European Union's Framework Programme for Research and Innovation HORIZON 2020 under grant agreement No 700395.

REFERENCES

[1] L. F. Ramos, L. Marques, P. B. Lourenço, G. De Roeck, A. Campos-Costa and J. Roque, "Monitoring of Historical Masonry Structures with Operation Modal Analysis: Two case studies," *Mechanical Systems and Signal Processing*, vol. 24, no. 5, pp. 1291-1305, July 2010.

[2] F. Ubertini, N. Cavalagli, A. Kita and G. Comanducci, "Assessment of a monumental masonry bell-tower after 2016 Central Italy seismic sequence by long-term SHM," *Bull Earthquake Eng, in press, DOI 10.1007/s10518-017-0222-7*, 2017.

[3] M. Tiritiello, *Analisi e modellazione numerica del campanile della Basilica di S. Pietro in Perugia, Master's Thesis*, University of Perugia, 2013.

[4] R. Vetturini, "DIVISARE," 9 January 2014. [Online]. Available: https://divisare.com/projects/247982-riccardo-vetturini-campanile-del-complesso-monumentale-di-s-pietro-in-perugia. [Accessed June 2017].

[5] F. Ubertini, C. Gentile and A. L. Materazzi, "Automated modal identification in operational conditions and its application to bridges," *Engineering Structures*, vol. 46, pp. 264-278, 2013.

[6] ICOMOS/ISCARSAH, "Recommendations for the Analysis, Conservation and Structural Restoration of Architectural Heritage," 2005.

[7] E. Manning, L. F. Ramos and F. Fernandes, "Direct Sonic and Ultrasonic Wave Velocity in Masonry under Compressive Stress," in *9th International Masonry Conference*, Guimarães, 2014.

[8] L. Miranda, J. Guedes, J. Rio and A. Costa, "Stone Masonry Characterization Through Sonic Tests," in *CINPAR 2010*, Cordoba, Argentina.

[9] F. Ubertini, N. Cavalagli, G. Comanducci and A. L. Materazzi, "Campanile di San Pietro," *L'Ingegnere Umbro*, pp. 7-13, June 2014.

[10] G. Comanducci, N. Cavalagli and F. Ubertini, "Vibration-based SHM for cultural heritage preservation: the case of the S. Pietro bell tower in Perugia," *MATEC Web of Conferences*, vol. 24, 2015.

[11] F. Ubertini, G. Comanducci, N. Cavalagli, A. L. Materazzi, A. L. Pisello and F. Cotana, "Automated post-earthquake damage detection in a monumental bell tower by continuous dynamic monitoring," in *Proceedings of the 10th International Conference on Structural Analysis of Historical Constructions, SAHC 2016*, Leuven, Belgium, Koen Van Balen & Els Verstrynge, 2016, pp. 812-819.

[12] F. Ubertini, G. Comanducci, N. Cavalagli, A. L. Pisello, A. L. Materazzi and F. Cotana, "Environmental effects on natural frequencies of the San Pietro bell tower in Perugia, Italy, and their removal for structural performance assessment," *Mechanical Systems and Signal Processing* , vol. 82, pp. 307-322, 2017.

[13] A. Saisi, C. Gentile and M. Guidobaldi, "Post-earthquake continuous dynamic monitoring of the Gabbia Tower in Mantua, Italy," *Construction and Building Materials*, vol. 81, pp. 101-112, 15 April 2015.

[14] L. F. Ramos, *Damage Identification on Masonry Structures Based on Vibration Signatures, PhD Thesis*, Universidade do Minho, 2007.